Parallel Pd Nanoribbons by Spontaneous Organization of Pd Nanoparticles

O. Taratula[*], A.M. Chen[*], J. Zhang[*], J. Chaudry[*], I. Banerjee[**] and H. He[*]

[*]Department of Chemistry, Rutgers University , 73 Warren street, Newark, NJ 07102, USA, huixinhe@newark.rutgers.edu

[**]Department of Chemistry, Fordham University, 441 East Fordham Road, Bronx, NY 10458, USA, bispsita@hotmail.com

ABSTRACT

A simple solution phase method was used to fabricate Pd nanoribbons which are composed by an array of Pd nanoparticles separated with nanometers gaps. A remarkable feature of this method is that no templates are required to produce the long uniform Pd nanoribbons. As a result the tedious separation and purification processes could be avoided. Furthermore, it is scalable for production of large quantity of Pd nanoribbons, which could be easily aligned and immobilized on insulating substrates for nanodevice fabrication.

Keywords: Pd, nanoribbons, nanoparticles, 1D assembly

1 INTRODUCTION

One dimensional (1D) assemblies of nanoparticles (NP) possess unique properties, stemming from synergetic coupling interactions between the nanoparticles [1]. These collective properties are not observed in their counterparts, individual nanoparticles, the bulk materials, or even 1D nanowires, which have an analogous morphology. The formation of highly anisotropic 1D NP assemblies and their associated collective properties are of enormous interest for the development of novel nanoelectronic, optoelectronic, nanomagnetic and biosensing devices. However, the 1D assemblies of NP are difficult to make because of the isotropic structure of 0D nanoparticles. Methods using hard and soft templates to guide the formation of 1D assemblies of NPs have been demonstrated [2,3]. However, the intrinsic disadvantages of the template methods are that the existence of the templates greatly influences the properties and applications of the produced 1D assemblies. In addition, removing the templates is difficult without destroying the integrity of the assembly [1]. Template free approaches are also reported to produce 1D NP assemblies by taking advantage of the intrinsic or induced magnetic and electronic dipoles [4]. However, most of the produced superstructures are branched 1D nanoparticle chain networks, which are difficult to be integrated for nanodevice fabrication. Nevertheless, without the guidance of templates, fabrication of straight and well-ordered one-dimensional assembly of nanoparticles is scant.

Since the discovery of semiconducting oxide nanobelts in 2001[5], belt-, ribbon-like nanomaterials have attracted considerable attention due to their distinctive geometry from nanowires, which could be used for a systematic understanding of dimensionally confined electrical, thermal, optical, and ionic transport processes in one-dimensional nanostructures. As a consequence, varieties of highly anisotropic and single crystalline nanobelts or ribbons have been fabricated [6]. However, to the best of our knowledge, no study has been reported on the preparation of ribbon-like nanoparticle assemblies.

In this work, we report a simple solution phase method to fabricate ribbon-shaped Pd nanoparticle assemblies. The Pd nanoribbons are so called because they have thickness of 6-10 nm, width of 60-100 nm and lengths up to hundred micrometers. These nanoribbons are composed of an array of Pd nanoparticles separated with nanometers gaps. This template-free method avoids the tedious separation and purification processes in the template-approaches. Furthermore, it can be scaled to produce a large quantity of Pd ribbons, and more importantly, the formed Pd nanoribbons can be easily aligned and immobilized on Si surfaces or other insulating substrates for future nanodevice fabrication.

2 EXPERIMENTAL SECTION

2.1 Materials

Palladium (II) acetate, tetraoctadecylammonium bromide, aminopropyl-triethoxysilane and 1-hexadecanethiol were purchased from Aldrich Chemicals Inc. Anhydrous tetrahydrofuran (THF) was purchased from Fisher, distilled from sodium/benzophenone prior to use. Toluene (HPLC grade, Alfa Aesar) and absolute ethanol (Pharmco) were used as received.

2.2 Preparation of Pd Nanoparticles

Pd nanoparticles, stabilized with tetraoctadecyl-ammonium bromide, were prepared according to previously established procedures [7]. Briefly, palladium (II) acetate (89.0 mM) and tetraoctadecylammonium bromide (22.5 mM) were dissolved in the mixture of toluene and tetrahydrofuran (5:1 v/v). After addition of absolute ethanol, the mixture was refluxed at 75 °C for 12 h. The color of the solution changed from yellow to deep brown-black indicating the formation of Pd nanoparticles. To initiate the precipitation of the colloids, an excess of

absolute ethanol was added slowly with vigorous shaking. Then the solution was decanted and the precipitate was dried under reduced pressure followed by mild heating. Finally, a gray-black powder was obtained and stored for Pd nanoribbons fabrication.

2.3 Atomic force Microscope (AFM)

The Pd nanoparticles and nanoribbons were imaged with tapping mode atomic force microscope in ambient air (Nanoscope III A, Digital Instruments). Conductive AFM measurements were performed by using a conductive diamond coated tip (Nanosensors).

2.4 Transmission Electron Microscope (TEM)

Images of the Pd nanoparticles and ribbons were taken using a JEOL 2100F 200kV FEG with 2kx2k CCD camera. One drop of the Pd solution was deposited on a carbon coated 200 mesh copper grid that was glow discharged for 1 minute. Excess liquid was removed using filter paper and the sample was viewed on the electron microscope.

2.5 X-ray Powder Diffraction (XRPD)

The X-ray powder diffraction pattern was generated on a Philips Analytical X'Pert PRO X-ray diffraction system with PW3040/60 console. A PW3373/00 ceramic Cu LEF X-ray tube Kα radiation was used as the source with an average wavelength of 1.54178 Å. The applied voltage and current were 40 kV and 50 mA, respectively. The powder samples were loaded onto a low-background silicon support plate and spread uniformly so that the sample surface was flat with the rim of the sample holder, which held the silicon support plate. In the case of the palladium nanoribbons, a drop of palladium nanribbon toluene solution was put onto the low-background silicon support and the sample after evaporation was analyzed by XRPD. The slight shift of the whole XRPD pattern due to the sample height change was corrected using the XRPD system software.

3 RESULTS AND DISCUSSION

3.1 Fabrication of Pd Nanoribbon Array

The first step of our approach involves the synthesis of tetraoctadecylammonium bromide stabilized Pd nanoparticles, which have the size in the range of 4.5 ± 0.2 nm (Figure 1a). The Pd nanoribbons were fabricated simply by dispersion of the palladium nanoparticle powder into toluene and incubated at room temperature for certain periods of time. Figure 1 shows that Pd nanoribbons with different lengths can be obtained by controlling the incubation time. The height (7 ± 1 nm) and width (75 ± 15 nm) of these ribbons did not change dramatically with longer incubation time.

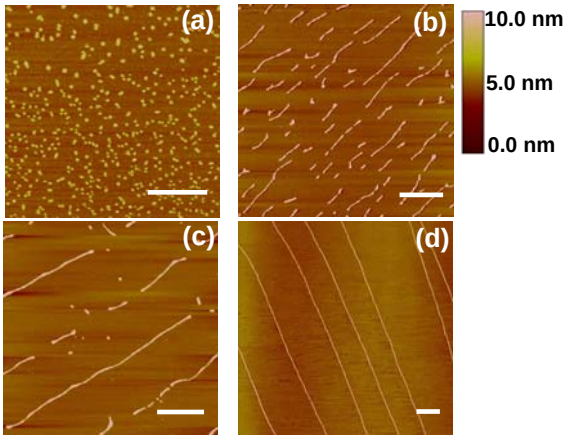

Figure 1: AFM images of Pd nanoparticles and nanoribbons with different incubation time: (a) 0, (b) 4, (c) 6, and (d) 24 days. The bars in the images represent 1.5 mm.

It is to be noted that using molecular combing technique, the ribbons are very easily aligned on mica or silicon surfaces to make a large array of parallel-arranged Pd nanoribbons with almost constant interline distances, indicating that the nanoribbons are formed in the solution phase. The production of highly aligned nanoribbons is compatible with the current microfabrication technology for device fabrication.

The growth of the ribbons can be discontinued or impeded significantly by introducing a stronger surfactant into the incubation solution, such as 1-hexadecanethiol ($CH_3(CH_2)_{15}SH$), which is known to strongly interact with Pd by the Pd-S bond [8]. After 6 days of incubation in toluene as shown in Figure 1c, the Pd solution was separated into two portions and 1 mM of 1-hexadecanethiol was introduced into only one portion of the solution.

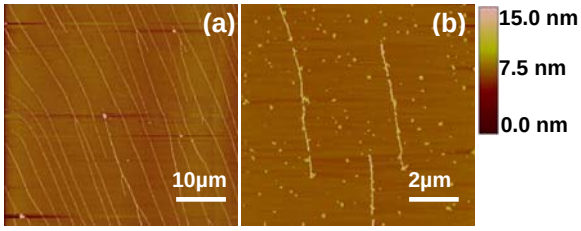

Figure 2: AFM images of Pd nanoribbons which were fabricated by (a) 24 days incubation in the original toluene solution, (b) 24 days incubation, however, 1 mM of $CH_3(CH_2)_{15}SH$ was introduced into the incubation solution on the sixth day of incubation.

Pd ribbons can grow as long as 100 μm after 24 days of incubation in the original toluene solution (Figure 2a.), however, the length of the Pd nanoribbons did not change very much after 24 days (Figure 2b). This result demonstrated that a strong surfactant is able to cease the

growth of the Pd ribbons so that it is possible to fabricate Pd nanoribbons with different lengths.

3.2 Morphology and crystal structure of the Pd nanoribbons

To shed light on the morphology of the fabricated Pd nanoribbons, high-resolution transmission electron microscopy (TEM) was used to study their inner structures. TEM images show that the nanoribbons are composed of isolated nanoparticles and necklace aggregates fused from the nanoparticles (Figure 3a). Most of the nanoparticles are separated with nanometer-sized gaps, which are possibly filled with the surfactant molecules. The fact that the Pd nanoribbons are composed of an array of Pd nanocrystals separated by nanogaps which results in their large electrical resistance (data not shown) is very encouraging for the preparation of high sensitive H_2 sensor based on the novel sensing principle developed by Penner et al [9].

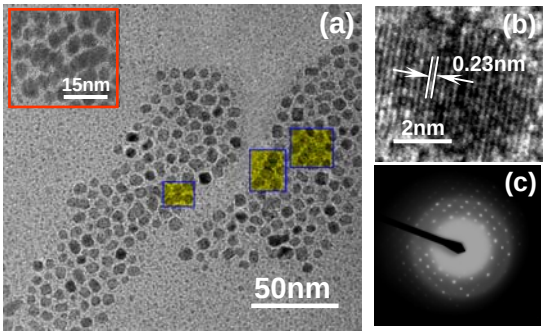

Figure 3: (a) TEM image of the Pd nanoribbons fabricated by 24 days incubation in toluene solution. (b) Lattice fringe structure of the nanoparticles in the nanoribbons. (c) Microdiffraction pattern of the individual nanoparticle.

The crystallographic structure of the Pd nanoparticles in the ribbon was determined with high resolution TEM as shown in Figure 3b and 3c. They normally possess {111} facets with a lattice fringe of approximately d_{111}= 0.23 ± 0.01 nm.

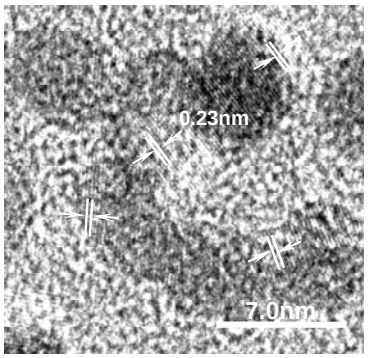

Figure 4: High-resolution TEM shows the attachment of the Pd nanoparticles.

It appears that Pd nanoparticles in the ribbons are aligned with a random orientation of the crystallographic faces. However, after fusion takes place, they prefer to orient themselves to have similar crystallographic facets in the ribbons as shown in Figure 4.

3.3 The organization mechanism

The exact mechanism of Pd nanoribbons formation is still under investigation. However, based on the experimental results, we can conclude that the formation of the nanoribbons is related to the partial removal of the surfactant, tetraoctadecylammonium bromide, which protecting the Pd particles from aggregation in the colloidal solution. Desorption of the surfactant from the particle's surface results in the increase of the attractive forces between particles, which allows them to align in certain direction [10].

X-ray powder diffraction (XRPD) experiments further support this presumption. Figure 5a shows the XRPD pattern of the Pd nanoparticles and the nanoribbons prepared from the nanoparticles. It is clear that both the Pd nanoparticles and the Pd ribbons possess crystal structures, with 111, 220, and 222 facets. A comparison of these two spectra shows the appearance of three sharp diffraction peaks at 2θ of 6.7, 11.0, 15.3° in the XRPD pattern of the nanoribbons. The same diffraction peaks have been observed in the XRPD spectrum of pure surfactant, tetraoctadecylammonium bromide (Figure 6b).

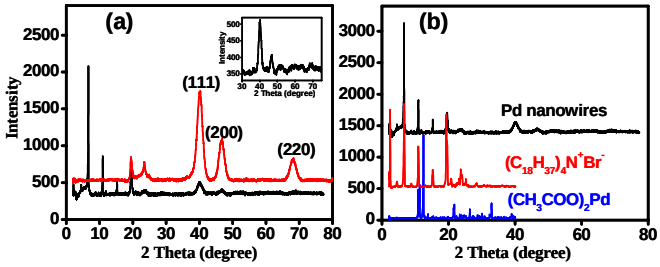

Figure 5: (a) XRD power patterns of the Pd nanoparticles and nanoribbons prepared from these nanoparticles after incubation in tolulene for 6 days. (Inset) Enlarged spectrum of Pd ribbons for clarity. (b) Comparison of the XRD power patterns between the Pd nanoribbons, pure surfactant, and Pd salts which were used during Pd nanoparticles preparation.

Therefore, the three sharp diffraction peaks shown in the Pd nanoribbon XRPD pattern are attributed to the crystalline surfactant of tetraoctadecylammonium bromide. Since the surfactant is adsorbed on the Pd nanoparticles surfaces, therefore, no diffraction peaks attributed to crystalline surfactant were present in the XRPD pattern of Pd nanoparticles. After incubation of the nanoparticles in toluene for 6 days, some of the surfactant molecules desorbed from the particle surface and dissolved in toluene solution. These surfactant molecules formed crystal structures during evaporation on the XRPD plate.

We have also found that slight change in the surfactant concentration during the Pd nanoparticles preparation dramatically influence the growing speed of the Pd nanoribbons (Figure 6). XRPD measurements show that in all cases, Pd nanoparticles with similar size (~4.5 nm) were obtained, although the amount of surfactant and its crystal structure in the powder are different. It is clear that the amount of the surfactant doesn't influence the size and the crystal structure of the Pd nanoparticles, however it does change the growing speed of Pd nanoribbons. As shown in Figure 7b, smaller amount of surfactant in the Pd powder results in the faster growing speed of the nanoribons. It can be understood that with larger amount of surfactant in the powder, the dynamic equilibrium of the surfactant between nanoparticles-bonded and free stabilizer becomes more difficult to shift toward its dissolved state, while Pd nanoribbons formation requires partially dissolution of the stabilizer from the Pd particles surface.

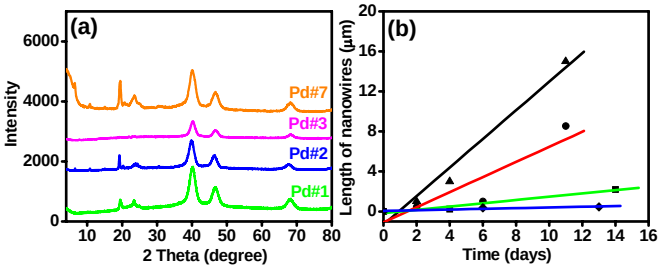

Figure 6. (a) XRD patterns of different batches of Pd nanowires. (b) Growth of the Pd nanoribbons from different batches of Pd powders.

Another factor which influences the growing speed of the Pd nanoribbons is the heat treatment during the drying process of Pd powder. Short time heating of Pd powder below 100°C can speed up the growth of the nanoribbons, while the drying at 100°C for 2 hrs largely slows down the growing speed. XRPD study of the heat-treated Pd powder reveals that the crystal structure and the size of the Pd particles don't change during the heat treatment. Therefore the different growing may be attributed to the increase in binding strength between the Pd surface and the surfactant after two hours heating at 100°C.

Another aspect to be considered is the fusion of the nanoparticles in quasi one direction to form the nanoribbons. The process of Pd nanoribbons fabrication is very similar to a recent report by Kotov et al. [11] for CdTe nanorods fabrication. One of the key steps in the preparation of nanorods from nanoparticles was the removal of excess stabilizer, which initiated the formation of necklace structures and finally resulted in the formation of luminescent nanowires. Analysis of the assembly mechanism of CdTe nanoparticles showed that the intrinsic dipole-dipole interaction between the nanoparticles was one of the primary forces in the formation of the 1D CdTe nanoparticles chains. Unlike semiconductor or other metal oxide nanoparticles, metallic nanoparticles exhibit no intrinsic electric dipole [3]. However, heterogeneity in surface charge and polarity associated, for example, with the non-uniform spatial distribution of the surfactant on different crystal facets is possible the driving force for anisotropic self-assembly. It is likely that the Pd nanoribbons also self-assemble in a similar manner. After the surfactant molecules are partially removed from the Pd nanoparticles, the asymmetrically distributed charges on the particle surfaces result in dipole interaction between the nanoparticles. In organic solvent, the nanoparticles are stabilized by the stronger interaction between the surfactant on the particles surface and the organic solvent molecules. When the induced dipole-dipole interaction is strong enough to overcome the thermal energy and the stronger interaction between the surfactant on the particles surface and the organic solvent molecules, the extrinsic electric dipole can lead to linear assembly.

In summary, a simple solution phase method to fabricate ribbon shaped Pd nanoparticle assemblies was reported. A remarkable feature of this approach is that no templates are required to produce the long uniform Pd nanoribbons. It is scalable for producing large quantities of Pd nanoribbons, and more importantly, the formed Pd nanoribbons can be easily aligned and immobilized on Si surfaces or other insulating substrates for future nanodevice fabrication. Due to the structural similarity to the Pd mesowires reported by Penner et al. [9], we expect that these nanoribbons can be readily used for developing novel H_2 sensors.

REFERENCES

[1] Tang, Z. Y.; Kotov, N. A. Adv. Mater. 2005, 17, 951-962.

[2] Yu, L.; Banerjee, I. A.; Shima, M.; Rajan, K.; Matsui, H. *Adv. Mater*. **2004,** *16*, 709-712.

[3] Ma, Y. F.; Zhang, J. M.; Zhang, G. J.; He, H. X. *J. Am. Chem. Soc.* **2004,** *126*, 7097-7101.

[4] Lin, S.; Li, M.; Dujardin, E.; Girard, C.; Mann, S. *Adv. Mater*. **2005,** *17*, 2553-2559.

[5] Pan, Z. W.; Dai, Z. R.; Wang, Z. L. *Science* **2001,** *291*, 1947.

[6] Joo, J.; Son, j. S.; Kwon, S. G.; Yu, J. H.; Hyeon, T. *J. Am. Chem. Soc.* **2006,** *128*, 5632.

[7] Hidber, P. C.; Nealey, P. F.; Helbig, W.; Whitesides, G. M. *Langmuir* **1996,** *12*, 5209-5215.

[8] Vyklicky, L.; Afzali-Ardakani, A.; Kagan, C. R. *Langmuir* **2005,** *21*, 11574-11577.

[9] Favier, F.; Walter, E. C.; Zach, M. P.; Benter, T.; Penner, R. M. *Science* **2001,** *293*, 2227.

[10] Korgel, B. A.; Fitzmaurice, D. *Advanced Materials* **1998,** *10*, (9), 661-665.

[11] Tang, Z. Y.; Kotov, N. A.; Giersig, M. *Science* **2003,** *297*, 237-240.